



ELSEVIER

Available online at www.sciencedirect.com

SCIENCE @ DIRECT®

Nuclear Instruments and Methods in Physics Research A 499 (2003) 469–479

**NUCLEAR
INSTRUMENTS
& METHODS
IN PHYSICS
RESEARCH**
Section A

www.elsevier.com/locate/nima

PHENIX detector overview

K. Adcox^a, S.S. Adler^b, M. Aizama^c, N.N. Ajitanand^d, Y. Akiba^e, H. Akikawa^f, J. Alexander^d, A. Al-Jamel^g, M. Allen^h, G. Alleyⁱ, R. Amirikas^j, L. Aphecetche^k, Y. Arai^e, J.B. Archuleta^l, J.R. Archuleta^l, R. Armendariz^g, V. Armijo^l, S.H. Aronson^b, D. Autrey^m, R. Averbeckⁿ, T.C. Awesⁱ, B. Azmounⁿ, A. Baldisseri^o, J. Banningⁱ, K.N. Barish^p, A.B. Barker^q, P.D. Barnes^l, J. Barrette^r, F. Barta^b, B. Bassalleck^s, S. Bathe^t, S. Batsouli^u, V.V. Baublis^v, A. Bazilevsky^{w,x}, R. Begayⁿ, J. Behrendt^s, S. Belikov^{y,z}, R. Belkin^b, F.G. Bellaicheⁱ, S.T. Belyaev^{aa}, M.J. Bennett^l, Y. Berdnikov^{ab}, S. Bhaganatula^z, J.C. Biggs^b, A.W. Bland^q, C. Blume^t, M. Bobrekⁱ, J.G. Boissevain^l, S. Boose^b, H. Borel^o, D. Borland^a, E. Bosze^p, S. Botelho^{ac}, J. Bowers^m, C. Brittonⁱ, L. Brittonⁱ, M.L. Brooks^l, A.W. Brown^q, D.S. Brown^g, N. Bruner^s, W.L. Bryanⁱ, D. Bucher^t, H. Buesching^t, V. Bumazhnov^w, G. Bunce^{b,x}, J. Burward-Hoyⁿ, S.A. Butsyk^{n,v}, M.M. Cafferty^l, T.A. Carey^l, J.S. Chai^{ad}, P. Chand^{ae}, J. Chang^p, W.C. Chang^{af}, R.B. Chappell^l, L.L. Chavez^s, S. Chernichenko^w, C.Y. Chi^u, J. Chiba^e, M. Chiu^u, S. Chollet^{ag}, R.K. Choudhury^{ae}, T. Christⁿ, T. Chujo^{b,c}, M.S. Chung^{ah,l}, P. Chung^d, V. Ciancioloⁱ, D.J. Clark^l, Y. Cobigo^o, B.A. Cole^u, P. Constantin^z, R. Conway^l, K.C. Cook^z, D.W. Crook^j, H. Cunitz^u, R. Cunningham^l, M. Cutshawⁱ, D.G. D'Enterria^k, C.M. Dabrowski^b, G. Danby^b, S. Danielsⁱ, A. Danmura^c, G. David^b, A. Debraine^{ag}, H. Delagrang^k, J. DeMoss^s, A. Denisov^w, A. Deshpande^x, E.J. Desmond^b, O. Dietzsch^{ac}, B.V. Dinesh^{ae}, J.L. Drachenberg^q, O. Drapier^{ag}, A. Dreesⁿ, R. du Rietz^{ai}, A. Durum^w, D. Dutta^{ae}, K. Ebisu^{aj}, M.A. Echave^l, Y.V. Efremenkoⁱ, K. El Chenawi^a, M.S. Emeryⁱ, D. Engo^b, A. Enokizono^{ak}, K. Enosawa^c, H. En'yo^{al,f}, N. Ericsonⁱ, S. Esumi^c, V.A. Evseev^v, L. Ewell^b, O. Fackler^m, J. Fellenstein^a, T. Ferdousi^p, J. Ferrierraⁿ, D.E. Fields^s, F. Fleuret^{ag}, S.L. Fokin^{aa}, B. Fox^x, Z. Fraenkel^{am}, S. Frankⁱ, A. Franz^b, J.E. Frantz^u, A.D. Frawley^j, J. Fried^b, J.P. Freidberg^{an}, E. Fujisawa^{ao}, H. Funahashi^f, S.-Y. Fung^p, S. Gadrat^{ap}, J. Gannon^b, S. Garpman^{ai}, F. Gastaldi^{ag}, T.F. Geeⁱ, R. Gentryⁱ, T.K. Ghosh^a, P. Giannotti^b, A. Glenn^h, A.L. Godoi^{ac}, M. Gonin^{ag}, G. Gogiberidze^h, J. Gosset^o, Y. Goto^x, R. Granier de Cassagnac^{ag}

*Corresponding author. Tel.: +1-515-294-6580; fax: +1-515-294-6027.

E-mail address: jhill@iastate.edu (J.C. Hill).

S.V. Greene^a, V. Griffin^j, M. Grosse Perdekamp^x, S.K. Gupta^{ae}, W. Guryn^b,
 H.-Å. Gustafsson^{ai}, T. Hachiya^{ak}, J.S. Haggerty^b, S. Hahn^l, J. Halliwellⁱ,
 H. Hamagaki^{aq}, R.H. Hance^q, A.G. Hansen^l, H. Hara^{aj}, J. Harder^b, G.W. Hart^l,
 E.P. Hartouni^m, A. Harvey^m, L. Hawkins^b, R.S. Hayano^{ar}, H. Hayashi^c,
 N. Hayashi^{al}, X. He^{as}, N. Heine^t, F. Heistermann^b, S. Held^h, T.K. Hemmickⁿ,
 J.M. Heuserⁿ, M. Hibino^{at}, J.S. Hicksⁱ, R. Higuchi^c, J.C. Hill^{z,*}, T. Hirano^c,
 D.S. Ho^{au}, R. Hoade^b, W. Holzmann^d, K. Homma^{ak}, B. Hong^{ah}, A. Hoover^g,
 T. Honaguchi^{x,ao}, C.T. Hunter^q, D.E. Hurstⁱ, R. Hutterⁿ, T. Ichihara^{al,x},
 V.V. Ikonnikov^{aa}, K. Imai^{f,al}, M. Inaba^c, M.S. Ippolitov^{aa}, L. Davis Isenhowe^q,
 L. Donald Isenhowe^q, M. Ishihara^{al,x}, M. Issah^d, V.I. Ivanov^v, B.V. Jacak^{n,x},
 G. Jacksonⁱ, J. Jackson^b, D. Jaffeⁱ, U. Jagadishⁱ, W.Y. Jang^{ah}, R. Jayakumar^{an},
 J. Jiaⁿ, B.M. Johnson^b, J. Johnsonⁱ, S.C. Johnson^{m,n}, J.P. Jonesⁱ, K. Jones^b,
 K.S. Joo^{av}, D. Jouan^{aw}, S. Kahn^b, F. Kajihara^{aq}, S. Kametani^{at}, N. Kamihara^{x,ao},
 Y. Kamyshev^{i,h}, A. Kandasamy^b, J.H. Kang^{au}, M.R. Kann^v, S.S. Kapoor^{ae},
 J. Kapustinsky^l, K.V. Karadjev^{aa}, V. Kashikhin^y, S. Kato^c, K. Katou^{at},
 H.-J. Kehayias^b, M.A. Kelley^b, S. Kelly^u, M. Kennedy^j, B. Khachaturov^{am},
 A.V. Khanzadeev^v, A. Khomutnikov^{ab}, J. Kikuchi^{at}, D.J. Kim^{au}, D.-W. Kim^{ax},
 G.-B. Kim^{ag}, H.J. Kim^{au}, S.Y. Kim^{au}, Y.G. Kim^{au}, W.W. Kinnison^l, E. Kistenev^b,
 A. Kiyomichi^c, C. Klein-Boesing^t, S. Klinksiek^s, L. Kluberg^{ag}, H. Kobayashi^x,
 V. Kochetkov^w, D. Koehler^s, T. Kohama^{ak}, B.G. Komkov^v, M.L. Kopytineⁿ,
 K. Koseki^c, L. Kotchenda^{v,ay}, D. Kotchetkov^p, Iou.A. Koutcheryaev^{aa},
 A. Kozlov^{am}, V.S. Kozlov^v, P.A. Kravtsov^v, P.J. Kroon^b, C.H. Kuberg^q,
 L.G. Kudin^v, M. Kurata-Nishimura^c, V.V. Kuriatkov^v, K. Kurita^{al,x}, Y. Kuroki^c,
 M.J. Kweon^{ah}, Y. Kwon^{au}, G.S. Kyle^g, J.J. LaBounty^b, R. Lacey^d, J.G. Lajoie^z,
 J. Lauret^d, A. Lebedev^z, V.A. Lebedev^{aa}, V.D. Lebedev^v, D.M. Lee^l, S. Lee^{ax},
 M.J. Leitch^l, M. Lenz^b, W. Lenz^b, X.H. Li^p, Z. Li^{az,al}, B. Libby^z, M. Libkind^m,
 W. Liccardi^b, D.J. Lim^{au}, S. Lin^b, M.X. Liu^l, X. Liu^{az}, Y. Liu^{aw}, Z. Liu^{az},
 E. Lockner^s, N. Longbotham^q, J.D. Lopez^l, R. Machnowski^b, C.F. Maguire^a,
 J. Mahon^b, Y.I. Makdisi^b, V.I. Manko^{aa}, Y. Mao^{az,al}, S. Marino^b, S.K. Mark^r,
 S. Markacs^u, D.G. Markushin^v, G. Martinez^k, X.B. Martinez^l, M.D. Marxⁿ,
 A. Masaike^f, F. Matathiasⁿ, T. Matsumoto^{aq,at}, P.L. McGaughey^l, M.C. McCain^q,
 J. Mead^b, E. Melnikov^w, Y. Melnikov^w, W.Z. Meng^b, M. Merschmeyer^t,
 F. Messerⁿ, M. Messer^b, Y. Miake^c, N.M. Miftakhov^v, S. Migluolio^{an}, J. Milan^d,
 T.E. Miller^a, A. Milov^{am}, K. Minuzzo^m, S. Mioduszewski^{b,h}, R.E. Mischke^l,
 G.C. Mishra^{as}, J.T. Mitchell^b, Y. Miyamoto^c, A.K. Mohanty^{ae}, B.C. Montoya^l,
 A. Mooreⁱ, T. Mooreⁱ, D.P. Morrison^b, G.G. Mosconeⁱ, J.M. Moss^l,
 F. Mühlbacherⁿ, M. Muniruzzaman^p, J. Murata^{al}, M.M. Murray^l, M. Musrockⁱ,
 S. Nagamiya^e, Y. Nagasaka^{aj}, J.L. Nagle^y, Y. Nakada^f, T. Nakamura^{ak},

B.K. Nandi^p, J. Negrin^b, J. Newby^h, L. Nikkinen^r, S.A. Nikolaev^{aa}, P. Nilsson^{ai},
 S. Nishimura^{aq}, A.S. Nyanin^{aa}, J. Nystrand^{ai}, E. O'Brien^b, P. O'Conner^b,
 F. Obenshainⁱ, C.A. Ogilvie^z, H. Ohnishi^{b,ak}, I.D. Ojha^{ba,a}, M. Ono^c, V. Onuchin^w,
 A. Oskarsson^{ai}, L. Österman^{ai}, I. Otterlund^{ai}, K. Oyama^{aq,ar}, L. Paffrath^b,
 A.P.T. Palounek^l, C.E. Pancakeⁿ, V.S. Pantuevⁿ, V. Papavassiliou^g, S.F. Pate^g,
 T. Peitzmann^t, R. Petersen^m, A.N. Petridis^z, C.H. Pinkenburg^{b,d}, R.P. Pisani^b,
 P. Pitukhin^w, T. Plagge^z, F. Plasilⁱ, M. Pollack^{n,h}, K. Pope^h, R. Prigl^b,
 M.L. Purschke^b, A.K. Purwarⁿ, J.M. Qualls^q, S. Rankowitz^b, G. Raoⁱ, R. Raoⁱ,
 M. Rau^b, I. Ravinovich^{am}, R. Raynis^b, K.F. Read^{i,h}, K. Reygers^t, G. Riabov^v,
 V.G. Riabov^{v,ab}, Yu.G. Riabov^v, S.H. Robinson^l, G. Roche^{ap}, A. Romana^{ag},
 M. Rosati^z, E.V. Roschin^v, A.A. Rose^a, P. Rosnet^{ap}, R. Roth^l, R. Ruggiero^b,
 S.S. Ryu^{au}, N. Saito^{al,x}, A. Sakaguchi^{ak}, T. Sakaguchi^{aq,at}, S. Sakai^c, H. Sako^c,
 T. Sakuma^{al,ao}, S. Salomoneⁿ, V.M. Samsonov^v, W.F. Sandhoff Jr.^b,
 L. Sanfratello^s, T.C. Sangster^m, R. Santo^t, H.D. Sato^{f,al}, S. Sato^c, R. Savino^b,
 S. Sawada^e, B.R. Schlei^l, R. Schleuter^{bb}, Y. Schutz^k, M. Sekimoto^e, V. Semenov^w,
 R. Seto^p, Y. Severgin^y, A. Shajii^{an}, V. Shangin^y, M.R. Shaw^q, T.K. Shea^b,
 I. Shein^w, V. Shelikhov^w, T.-A. Shibata^{al,ao}, K. Shigaki^e, T. Shiina^l, T. Shimada^c,
 Y.H. Shin^{au}, I.G. Sibiriak^{aa}, D. Silvermyr^{ai}, K.S. Sim^{ah}, J. Simon-Gillo^l,
 M. Simpsonⁱ, C.P. Singh^{ba}, V. Singh^{ba}, W. Sippach^u, M. Sivertz^b, H.D. Skank^z,
 S. Skutnik^z, G.A. Sleege^z, D.C. Smithⁱ, G.D. Smith^l, M. Smithⁱ, A. Soldatov^w,
 G.P. Solodov^v, R.A. Soltz^m, W.E. Sondheim^l, S. Sorensen^{i,h}, I. Sourikova^b,
 F. Staley^o, P.W. Stankusⁱ, N. Starinsky^r, S. Steffens^h, E.M. Stein^b, P. Steinberg^u,
 E. Stenlund^{ai}, M. Stepanov^g, A. Ster^{bc}, J. Stewering^t, W. Stokes^b, S.P. Stoll^b,
 M. Sugioka^{al,ao}, T. Sugitate^{ak}, J.P. Sullivan^l, Y. Sumi^{ak}, Z. Sun^{az},
 M. Suzuki-Nara^c, E.M. Takagui^{ac}, A. Taketani^{al}, M. Tamai^{at}, K.H. Tanaka^e,
 Y. Tanaka^{aj}, E. Taniguchi^{al,ao}, M.J. Tannenbaum^b, V.I. Tarakanov^v,
 O.P. Tarasenkova^v, J.D. Tepe^q, R. Thern^b, J.H. Thomas^m, J.L. Thomasⁿ,
 T.L. Thomas^s, W.D. Thomas^z, G.W. Thornton^l, W. Tian^{az,h}, R. Toddⁱ, J. Tojo^{f,al},
 F. Toldo^b, H. Torii^{f,al}, R.S. Towell^{q,l}, J. Tradeski^b, V.A. Trofimov^v, I. Tserruya^{am},
 H. Tsuruoka^c, A.A. Tsvetkov^{aa}, S.K. Tuli^{ba}, G. Turnerⁱ, H. Tydesjö^{ai}, N. Tyurin^w,
 S. Urasawa^c, A. Usachev^w, T. Ushiroda^{aj}, H.W. van Hecke^l, M. Van Lith^b,
 A.A. Vasiliev^{aa}, V. Vasiliev^y, M. Vassent^{ap}, C. Velissaris^g, J. Velkovskaⁿ,
 M. Velkovskyⁿ, W. Verhoeven^t, L. Villatte^h, A.A. Vinogradov^{aa}, V.I. Vishnevskii^v,
 M.A. Volkov^{aa}, W. Von Achen^b, A.A. Vorobyov^v, E.A. Vznuzdaev^v,
 M. Vznuzdaev^v, J.W. Walkerⁱ, Y. Wan^{az}, H.Q. Wang^p, S. Wang^j, Y. Watanabe^{al,x},
 L.C. Watkinsⁱ, T. Weimer^z, S.N. White^b, B.R. Whitusⁱ, C. Williamsⁱ, P.S. Willis^q,
 A.L. Wintenbergⁱ, C. Witzig^b, F.K. Wohn^z, K. Wolniewicz^b,
 B.G. Wong-Swanson^l, L. Wood^z, C.L. Woody^b, L.W. Wright^j, J. Wuⁿ, W. Xie^{p,am},

N. Xu^h, K. Yagi^c, R. Yamamoto^m, Y. Yang^{b,az}, S. Yokkaichi^{al}, Y. Yokota^c,
S. Yoneyama^{ao}, G.R. Youngⁱ, I.E. Yushmanov^{aa}, W.A. Zajc^u, C. Zhang^u,
L. Zhang^u, Z. Zhangⁿ, S. Zhou^{az}

^a Vanderbilt University, Nashville, TN 37235, USA

^b Brookhaven National Laboratory, Upton, NY 11973-5000, USA

^c Institute of Physics, University of Tsukuba, Tsukuba, Ibaraki 305, Japan

^d Chemistry Department, State University of New York—Stony Brook, Stony Brook, NY 11794, USA

^e KEK, High Energy Accelerator Research Organization, Tsukuba-shi, Ibaraki-ken 305-0801, Japan

^f Kyoto University, Kyoto 606, Japan

^g New Mexico State University, Las Cruces, NM 88003, USA

^h University of Tennessee, Knoxville, TN 37996, USA

ⁱ Oak Ridge National Laboratory, Oak Ridge, TN 37831, USA

^j Florida State University, Tallahassee, FL 32306, USA

^k SUBATECH (Ecole des Mines de Nantes, IN2P3/CNRS, Universite de Nantes) BP 20722-44307, Nantes Cedex 3, France

^l Los Alamos National Laboratory, Los Alamos, NM 87545, USA

^m Lawrence Livermore National Laboratory, Livermore, CA 94550, USA

ⁿ Department of Physics and Astronomy, State University of New York - Stony Brook, Stony Brook, NY 11794, USA

^o DSM/Dapnia/SPH, CEA/Saclay, 91191 Gif-sur-Yvette Cedex, France

^p University of California—Riverside, Riverside, CA 92521, USA

^q Abilene Christian University, Abilene, TX 79699, USA

^r McGill University, Montreal, Que., Canada H3A 2T8

^s University of New Mexico, Albuquerque, NM 87131, USA

^t Institut für Kernphysik, University of Münster, D-48149 Münster, Germany

^u Columbia University, New York, NY 10027 and Nevis Laboratories, Irvington, NY 10533, USA

^v PNPI, Petersburg Nuclear Physics Institute, Gatchina, Russia

^w Institute for High Energy Physics (IHEP), Protvino, Russia

^x RIKEN BNL Research Center, Brookhaven National Laboratory, Upton, NY 11973-5000, USA

^y Efremov Institute for Electrophysical Research, St. Petersburg, Russia

^z Iowa State University, Ames, IA 50011, USA

^{aa} Russian Research Center “Kurchatov Institute”, Moscow, Russia

^{ab} St. Petersburg State Technical University, St. Petersburg, Russia

^{ac} Universidade de São Paulo, Instituto de Física, Caixa Postal 66318, São Paulo CEP05315-970, Brazil

^{ad} C.A.L., Korea Cancer Hospital, Seoul 139-706, South Korea

^{ae} Bhabha Atomic Research Centre, Bombay 400 085, India

^{af} Institute of Physics, Academia Sinica, Taipei 11529, Taiwan

^{ag} L.L.R., Ecole Polytechnique, 91128 Palaiseau, France

^{ah} Korea University, Seoul 136-701, South Korea

^{ai} Department of Physics, Lund University, Box 118, SE-221 00 Lund, Sweden

^{aj} Nagasaki Institute of Applied Science, Nagasaki-shi, Nagasaki 851-0193, Japan

^{ak} Hiroshima University, Kagamiyama, Higashi-Hiroshima 739-8526, Japan

^{al} RIKEN (The Institute of Physical and Chemical Research), Wako, Saitama 351-0198, Japan

^{am} Weizmann Institute, Rehovot 76100, Israel

^{an} Plasma Science and Fusion, Center Massachusetts Institute of Technology, Cambridge, MA 02139, USA

^{ao} Department of Physics, Tokyo Institute of Technology, Tokyo, 152-8551, Japan

^{ap} L.P.C., Université Blaise Pascal, 63177 Aubiere Cedex, France

^{aq} Center for Nuclear Study, Graduate School of Science, University of Tokyo, 7-3-1 Hongo, Bunkyo, Tokyo 113-0033, Japan

^{ar} University of Tokyo, Tokyo, Japan

^{as} Georgia State University, Atlanta, GA 30303, USA

^{at} Waseda University, Advanced Research Institute for Science and Engineering, 17 Kikui-cho, Shinjuku-ku, Tokyo 162-0044, Japan

^{au} Yonsei University, IPAP, Seoul 120-749, South Korea

^{av} Myongji University, Yongin, Kyonggido 449-728, South Korea

^{aw} I.P.N., BP 1, 91406 Orsay, France

^{ax} Kangnung National University, Kangnung 210-702, South Korea

^{ay} State Interphysica, Protvino, Russia

^{az} China Institute of Atomic Energy (CIAE), Beijing, People's Republic of China

^{ba} Department of Physics, Banaras Hindu University, Varanasi 221005, India^{bb} Lawrence Berkeley National Laboratory, Berkeley, CA 94720, USA^{bc} KFKI Research Institute for Particle and Nuclear Physics (RMKI), Budapest, Hungary

The PHENIX Collaboration

Abstract

The PHENIX detector is designed to perform a broad study of A–A, p–A, and p–p collisions to investigate nuclear matter under extreme conditions. A wide variety of probes, sensitive to all timescales, are used to study systematic variations with species and energy as well as to measure the spin structure of the nucleon. Designing for the needs of the heavy-ion and polarized-proton programs has produced a detector with unparalleled capabilities. PHENIX measures electron and muon pairs, photons, and hadrons with excellent energy and momentum resolution. The detector consists of a large number of subsystems that are discussed in other papers in this volume. The overall design parameters of the detector are presented.

© 2002 Elsevier Science B.V. All rights reserved.

PACS: 25.75.–q; 29.30.–h; 29.40.–n

Keywords: RHIC; PHENIX; Heavy ions; Spectrometer

1. Introduction

The Relativistic Heavy Ion Collider (RHIC) at Brookhaven National Laboratory accelerates nuclear beams from protons to gold. For the heaviest beams an energy of 100 GeV/nucleon is reached. Four detectors, BRAHMS, PHENIX, PHOBOS and STAR, are operating to study collisions ranging from p–p to Au–Au. The Pioneering High Energy Nuclear Interaction eXperiment (PHENIX) is carried out by a collaboration of about 500 physicists and engineers from 54 participating institutions in 13 countries [1]. Fig. 1 shows a subset of the Collaboration standing in front of parts of the PHENIX detector.

The PHENIX experiment probes several fundamental features of the strong interaction. A prime goal for experiments with heavy ion beams is to produce a deconfined state of nuclear matter called the Quark Gluon Plasma (QGP) and study its properties. This is thought to be the state of the universe a μs after its birth in the “big bang”. Measuring leptons and photons probes the QGP phase directly, while studying the copiously produced hadrons gives information on the later hadronization of the QGP. RHIC also provides

the opportunity to study collisions of polarized protons. The aim is to measure the spin structure of the nucleon [2].

In order to carry out this broad physics agenda the PHENIX detector utilizes a variety of detector technologies. It uses global detectors to characterize the collisions, a pair of central spectrometers at mid-rapidity to measure electrons, hadrons, and photons, and a pair of forward spectrometers to measure muons. Each spectrometer has a large geometric acceptance of about one steradian and excellent energy and momentum resolution and particle identification.

2. Physics goals of PHENIX

Quantum Chromodynamics (QCD) predicts that heavy nuclei colliding at ultrarelativistic energies will undergo a phase transition from hadronic matter to a deconfined state of quarks and gluons moving freely over a volume approximately 10 fm^3 , namely the QGP.

This process can be thought of as proceeding through a series of steps from the initial collision through QGP formation (deconfinement) and



Fig. 1. Members of the PHENIX collaboration in front of the PHENIX detector.

possible chiral symmetry restoration. The QGP would thermalize followed by expansion and cooling leading to hadronization. PHENIX is able to probe each phase of the above process by virtue of its ability to study the rare processes involving photons, electrons and muons as well as the predominant hadronic production. The experiment has a high rate capability and fine granularity combined with excellent momentum, energy and mass resolution.

Direct photons and lepton pairs which emerge from the collision with a minimum of final state interaction are sensitive to the full time evolution from the initial state through thermalization. The capability to measure direct photons over a wide range of p_T is unique to PHENIX and is important for relating their momentum to the temperature of the emitting source.

Jets from the hard scattering of constituent quarks and gluons are produced in the initial state and are sensitive to the properties of the medium during the evolution so that a significant modification of the structure of the jet is expected if a QGP

is formed. PHENIX studies the deconfined state and Debye screening by observing the yields of the J/Ψ and Ψ' relative to that of the Υ . Chiral symmetry restoration is predicted to result in the reduction of quark masses and possible changes in the lifetime and width of the ϕ and possibly the ρ and ω . All of the above vector mesons are studied by observation of their decays into lepton pairs.

After hadronization the expansion of the fireball is studied by measurement of Hanbury–Brown–Twiss correlations and the coalescence probabilities of various nuclei and anti-nuclei give insights into the space-time evolution of the collision. Precision time-of-flight (ToF) allows measurement of the identified charged hadron spectrum over a wide p_T range. Many of the above signals can also be produced from interactions between particles in hot hadronic matter. It is thus necessary to understand the purely hadronic effects. For this reason PHENIX studies the above signals using p–p and p–A collisions to gain a better understanding of effects distorting signals from the QGP.

A second major goal of the PHENIX experiment is to measure the spin structure of the nucleon. RHIC accelerates beams of polarized protons up to 250 GeV with polarizations up to 50%. Work of the EMC [3] collaboration and others indicated that the fraction of the proton spin carried by the quarks was only about half of the expected value. PHENIX studies the gluon polarization by measuring high p_T prompt photon production using the highly segmented EM Calorimeter to minimize interference from photons from π^0 decays. The anti-quark polarization is measured by observing the parity violating asymmetry for W production. The W particles are identified by the detection of muons or electrons with $p_T \geq 20$ GeV/c using the PHENIX north and south muon arms or the central spectrometer, respectively.

3. PHENIX detector subsystems

The PHENIX detector comprises four instrumented spectrometers or arms and three global detectors [4]. The detector consists of a number of subsystems. The rapidity and ϕ coverages and other features of these subsystems is given in Table 1 and a perspective drawing of the PHENIX detector with the major subsystems labeled is shown in Fig. 2. Also an overview of the subsystems is given below. The east and west central arms are centered at zero rapidity and instrumented to detect electrons, photons and charged hadrons. The north and south forward arms have full azimuthal coverage and are instrumented to detect muons. Each of the four arms has a geometric acceptance of approximately one steradian. The global detectors measure the start time, vertex and multiplicity of the interactions. A photograph of the PHENIX detector from above is shown in Fig. 3.

3.1. Global detectors

In order to characterize the nature of an event following a heavy ion collision, three global detectors are employed. They consist of Zero-Degree Calorimeters (ZDC), Beam-Beam Coun-

ters (BBC) and the Multiplicity-Vertex Detector (MVD). A pair of ZDCs [5] detect neutrons from grazing collisions and form a trigger for the most peripheral collisions. The ZDC is used by all four RHIC detectors and is discussed elsewhere in this volume [6]. A pair of BBCs [7] provide a measure of the ToF of forward particles to determine the time of a collision, provide a trigger for the more central collisions and provide a measure of the collision position along the beam axis. The MVD [7] provides a more precise determination of event position and multiplicity and measures fluctuations of the charged particle distributions. It is composed of concentric barrels of silicon-strip detectors and endcaps made of silicon pads. Recently a Normalization Trigger Counter (NTC) [7] has been added between the MVD endcaps and the central magnet pole tips. The NTC extends the coverage of the BBC for p-p and p-A running.

3.2. Central spectrometers

The magnetic field for the central spectrometer is supplied by the central magnet [8] that provides an axial field parallel to the beam and around the interaction vertex. The central arms consist of tracking systems for charged particles and electromagnetic calorimetry. The calorimeter [9] is the outermost subsystem on the central arms and provides measurements of both photons and energetic electrons. A lead-scintillator (PbSc) calorimeter is used for good timing and a lead-glass (PbGl) calorimeter gives good energy resolution.

The tracking system uses three sets of Pad Chambers (PC) [10] to provide precise three-dimensional space points needed for pattern recognition. The precise projective tracking of the drift chambers (DC) [10] is the basis of the excellent momentum resolution. A Time Expansion Chamber (TEC) [10] in the east arm provides additional tracking and particle identification. The ToF and Ring-Imaging Cherenkov (RICH) detectors also provide particle identification [11]. The 85 ps timing resolution of the ToF allows separation of kaons from pions up to 2.5 GeV/c and proton identification out to 5 GeV/c. For p-p

Table 1
Summary of the PHENIX detector subsystems

Element	$\Delta\eta$	$\Delta\phi$	Purpose and special features
<i>Magnet</i>			
Central (CM)	± 0.35	360°	Up to 1.15 T m
Muon (MMS)	-1.1 – 2.2	360°	0.72 T m for $\eta = 2$
Muon (MMN)	1.1 – 2.4	360°	0.72 T m for $\eta = 2$
Silicon (MVD)	± 2.6	360°	$d^2N/d\eta d\phi$, precise vertex, Reaction plane determination
Beam–beam (BBC)	$\pm(3.1$ – $3.9)$	360°	Start timing, fast vertex
NTC	$\pm(1$ – $2)$	320°	Extend coverage of BBC for p–p and p–A
ZDC	± 2 mrad	360°	Minimum bias trigger
Drift chambers (DC)	± 0.35	$90^\circ \times 2$	Good momentum and mass resolution $\Delta m/m = 1.0\%$ at $m = 1$ GeV
Pad chambers (PC)	± 0.35	$90^\circ \times 2$	Pattern recognition, tracking for nonbend direction
TEC	± 0.35	90°	Pattern recognition, dE/dx Good momentum resolution for $p_T > 4$ GeV/c
RICH	± 0.35	$90^\circ \times 2$	Electron identification
ToF	± 0.35	45°	Good hadron identification, $\sigma < 100$ ps
T0	± 0.35	45°	Improve ToF timing for p–p and p–A
PbSc EMCal	± 0.35	$90^\circ + 45^\circ$	For both calorimeters, photon and electron detection and energy measurement
PbGl EMCal	± 0.35	45°	Good e^\pm/π^\pm separation at $p > 1$ GeV/c by EM shower and $p < 0.35$ GeV/c by ToF K^\pm/π^\pm separation up to 1 GeV/c by ToF
<i>μ tracker</i>			
(μ TS)	-1.15 to -2.25	360°	Tracking for muons
(μ TN)	1.15 to 2.44	360°	Muon tracker north installed for year-3
<i>μ identifier</i>			
(μ IDS)	-1.15 to -2.25	360°	Steel absorbers and Iarocci tubes for muon/hadron separation
(μ IDN)	1.15 to 2.44	360°	

running the ToF timing resolution would be poorer than for heavy ions due to a reduced number of particles in the BBC. The ToF timing is improved by the use of a T0 counter [11] outside the barrel of the MVD. This is needed for p–p and p–A experiments. The RICH provides separation of electrons from the large number of copiously produced pions. Using information from the RICH, the TEC and the electromagnetic calorimeter it is possible to reject pion contamination of identified electrons to one part in 10^4 over a wide range of momentum.

3.3. Muon spectrometers

The two forward muon spectrometers [12] give PHENIX acceptance for J/Ψ decaying into dimuons at rapidities of $-2.25 \leq y \leq -1.15$ for the south arm and $1.15 \leq y \leq 2.44$ for the north arm. Each spectrometer is based on a muon tracker inside a radial magnetic field [8] followed by a muon identifier, both with full azimuthal acceptance. The muon trackers consist of three stations of multi-plane drift chambers that provide precision tracking. The muon identifiers consist of

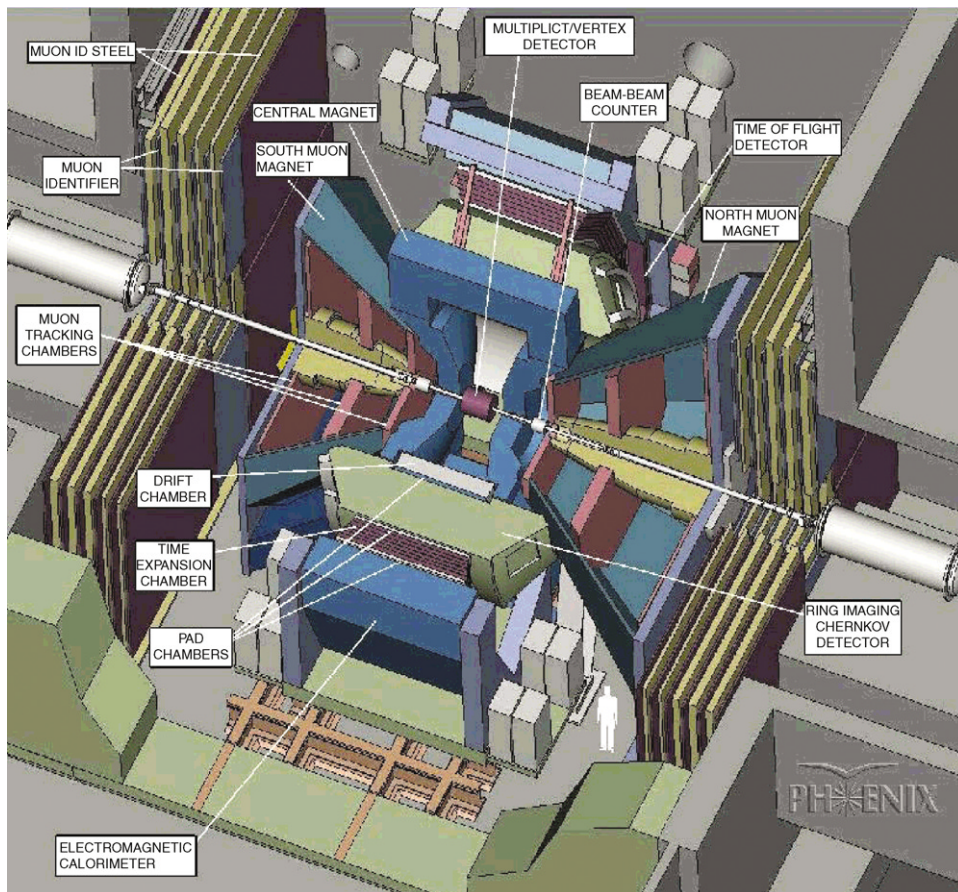


Fig. 2. A cutaway drawing of the PHENIX detector. Labeled arrows point to the major detector subsystems.

alternating layers of steel absorbers and low resolution tracking layers of streamer tubes of the Iarocci type. With this combination the pion contamination of identified muons is typically 3×10^{-3} . The complete north arm will be installed prior to the year-3 PHENIX run.

3.4. Electronics and computing

PHENIX selects and archives events of potential physics interest at the maximum rate consistent with the available RHIC luminosity. The channel count for the PHENIX detector is large and details for the various subdetectors is given in Table 2. Note that for some subsystems two ADCs are required per channel to get the needed dynamic range. In order to obtain a high data-collection

efficiency a high degree of coordination between the electronics and computing efforts is required. Custom Front-End Electronics (FEE) were designed for the PHENIX subsystems. Signals from the FEEs [13] are transported by optical fibers to the level-1 trigger [13] that processes signals from a number of subsystems and then either accepts or rejects the event. The trigger operates in a synchronous pipelined mode with a latency of 40 beam crossings, and thus generates a decision for each crossing. The timing of the above operations is coordinated by a master timing system [13] that distributes the RHIC clocks to granule timing modules that communicate with the FEEs.

In order to study the rare event physics for which PHENIX was designed, it is necessary to have a higher level of event rejection than possible

with the level-1 trigger alone. Therefore a level-2 software trigger [13] that makes its selection after a complete event is assembled was developed.

Table 2

Channel counts, digitizer channels and LVL-1 trigger bits/sums for PHENIX

Subsystem symbol	Detector channels	ADC channels	TDC channels	LVL-1 inputs
BB	128	128	256	128 bits
MVD	20,736	20,736		
NTC	8	8	16	8 bits
DC	12,800		12,800	
PC	172,800		172,800	
TEC	20,480	20,480		
RICH	5120	5120	5120	256 bits
ToF	1920	1920	1920	1920 bits
T0	22	22	44	22 bits
EMCal	24,768	49,536	24,768	688 bits
μ TR	43,968	43,968		
μ ID	6340		6340	6340 bits

Once the level-1 trigger accepts an event, the data from the various subsystems is routed via fiber-optic cable to the data collection modules [13]

Table 3

Performance of the PHENIX detector

Physics	Year-2 version
Electrons	$\pi/e < 10^{-4}$ at $p \leq 4.7$ GeV/c RICH for < 4.7 GeV/c TEC (dE/dx) for < 2 GeV/c EMCal for > 0.5 GeV/c
Photons	$p_T \geq 1$ GeV/c for 0.5 sr with PbGl $p_T \geq 1$ GeV/c for 1.5 sr with PbSc Single γ s resolved from merging $\pi^0 \rightarrow \gamma + \gamma$ out to $p_T \geq 25$ GeV/c
Hadrons	≤ 2.3 GeV/c π for 0.38 sr ≤ 1.6 GeV/c K for 0.38 sr ≤ 5.0 GeV/c p for 0.38 sr ToF with $\sigma < 100$ ps
Muons	$\pi/\mu < 3 \times 10^{-3}$ at $p \geq 2.3$ GeV/c with 5 layers of μ ID.
Global	$d^2N/d\eta d\phi$ for $ \eta < 2.6$

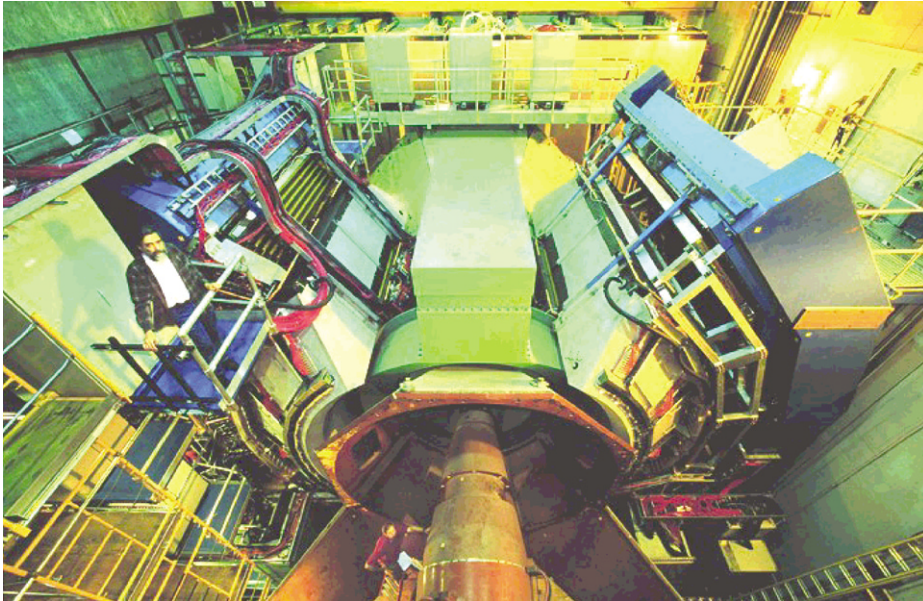


Fig. 3. Photograph of the PHENIX detector viewed from north to south. The central arms are visible on the right (west) and east (left) sides. In the back the south muon magnet and the muon identifier detectors are visible.

that interact with the subsystems by means of daughter cards that format and zero-suppress the data. Data packets are generated by digital signal processors and sent to event builders [13] that assemble the events in their final form. The control and monitoring of the electronics and triggering is handled by the On-Line Computing System (ONCS) [14]. ONCS configures and initializes the on-line system, monitors and controls the data flow and interlocks the data acquisition process with the slow controls systems. After the data is collected the off-line system [14] provides event reconstruction, data analysis and information management. It provides the tools to convert raw data into physics results.

4. Conclusion

The performance of the PHENIX detector is summarized in Table 3. It is designed to carry out the broadest possible study of collisions from Au–Au to p–p. The goal is to examine nuclear matter under a variety of extreme conditions using a variety of probes sensitive to all time scales. In addition, studies of various signals are carried out as a function of both energy and nuclear species in order to separate QGP signals from those of hadronic origin. Another goal is to measure the spin structure of the nucleon by determining the contributions from anti-quarks and gluons. The above goals have resulted in the production of a detector with unparalleled capabilities. In the summer of 2000 a number of Au–Au collisions were observed between Au ions with energies of 65 GeV/nucleon using the central spectrometer. In the first PHENIX physics publication [15] results from the measurement of the charged-particle multiplicity are presented. Subsequently results from the first measurement of energy transverse to the beam direction [16], on mass dependence of two-pion correlations [17], on measurement of single electrons with implications for charm production [18] and on the centrality dependence of pion, kaon, proton and antiproton production [19] have been published and studies of results from Au–Au collisions with 100 GeV/nucleon beams are underway.

Acknowledgements

We thank the staff of the RHIC project, Collider-Accelerator, and Physics Departments at BNL and the staff of PHENIX participating institutions for their vital contributions. We acknowledge support from the Department of Energy and NSF (USA), Monbu-sho and STA (Japan), RAS, RMAE, and RMS (Russia), BMBF and DAAD (Germany), FRN, NFR, and the Wallenberg Foundation (Sweden), MIST and NSERC (Canada), CNPq and FAPESP (Brazil), IN2P3/CNRS and DAPNIA/CEA (France), DAE (India), KRF and KOSEF (Korea) and the US–Israel Binational Science Foundation.

References

- [1] Y. Akiba, et al., Nucl. Phys. A 638 (1998) 565c.
- [2] N. Saito, et al., Nucl. Phys. A 638 (1998) 575c.
- [3] J. Ashman, et al. (EM Collaboration), Phys. Lett. B 202 (1988) 603;
J.J. Aubert, et al. (EM Collaboration), Phys. Lett. B 123 (1983) 275.
- [4] PHENIX Conceptual Design Report, BNL, 1993, unpublished.
- [5] C. Adler, et al., Nucl. Instr. and Meth. A 470 (2001) 488.
- [6] ZDC article, Nucl. Instr. and Meth. A (2003), this issue.
- [7] M. Allen, et al., PHENIX inner detectors, Nucl. Instr. and Meth. A (2003), this issue.
- [8] S.M. Aronson, et al., PHENIX magnet system, Nucl. Instr. and Meth. A (2003), this issue.
- [9] L. Aphecetche, et al., PHENIX calorimeter, Nucl. Instr. and Meth. A (2003), this issue.
- [10] K. Adcox, et al., PHENIX central arm tracking detectors, Nucl. Instr. and Meth. A (2003), this issue.
- [11] M. Aizawa, et al., PHENIX central arm particle ID detectors, Nucl. Instr. and Meth. A (2003), this issue.
- [12] H. Akikawa, et al., PHENIX muon arms, Nucl. Instr. and Meth. A (2003), this issue.
- [13] S.S. Adler, et al., PHENIX on-line systems, Nucl. Instr. and Meth. A (2003), this issue.
- [14] S.S. Adler, et al., PHENIX on-line and off-line computing, Nucl. Instr. and Meth. A (2003), this issue.
- [15] K. Adcox, et al., Phys. Rev. Lett. 86 (2001) 3500.
- [16] K. Adcox, et al., Phys. Rev. Lett. 87 (2001) 052301.
- [17] K. Adcox, et al., Phys. Rev. Lett. 88 (2002) 192302.
- [18] K. Adcox, et al., Phys. Rev. Lett. 88 (2002) 192303.
- [19] K. Adcox, et al., Phys. Rev. Lett. 88 (2002) 242301.